Bioorganic & Medicinal Chemistry Letters 22 (2012) 5257–5263

Contents lists available at SciVerse ScienceDirect

Bioorganic & Medicinal Chemistry Letters

journal homepage: www.elsevier.com/locate/bmcl

SAR studies around a series of triazolopyridines as potent and selective PI3Kγ inhibitors

Kathryn Bell [a,*], Mihiro Sunose [a], Katie Ellard [a], Andrew Cansfield [a], Jess Taylor [a], Warren Miller [a], Nigel Ramsden [a], Giovanna Bergamini [b], Gitte Neubauer [b]

[a] Cellzome Ltd, Chesterford Research Park, Cambridge, CB10 1XL, United Kingdom
[b] Cellzome AG, Meyerhofstr. 1, 69117 Heidelberg, Germany

ARTICLE INFO

Article history:
Received 4 May 2012
Revised 14 June 2012
Accepted 15 June 2012
Available online 23 June 2012

Keywords:
PI3Kγ
Kinase inhibitor
Inflammation
Triazolopyridine
Collagen induced arthritis

ABSTRACT

Herein we describe the SAR of a novel series of 6-aryl-2-amino-triazolopyridines as potent and selective PI3Kγ inhibitors. The 6-aryl-triazolopyridine core was identified by chemoproteomic screening of a kinase focused library. Rapid chemical expansion around a bi-functional core identified the key features required for PI3Kγ activity and selectivity. The series was optimized to afford **43** (CZC19945), a potent PI3Kγ inhibitor with high oral bioavailability and selectivity over PI3Kα and PI3Kδ. Modification to the core afforded **53** (CZC24832) which showed increased selectivity over the entire kinome in particular over PI3Kβ.

Phosphoinositide 3-kinase γ (PI3Kγ) is one of four Class I PI3Ks, a family of dual lipid and protein kinases involved in the regulation of numerous biological processes, including cell growth, differentiation, survival, proliferation and migration.[1] Class IA comprises PI3Kα, PI3Kβ and PI3Kδ, while PI3Kγ is the sole member of Class IB. PI3Kγ plays a key role in immune responses such as immune cell migration[2] and mast cell degranulation,[3] and the genetic or pharmacological inactivation of its kinase activity confers protection in murine models of inflammatory diseases.[4] PI3Kα and PI3Kβ are key mediators of insulin signaling[5] and are necessary during development as genetic inactivation results in embryonic lethality.[6,7] On the other hand, PI3Kγ knock-out mice are viable, fertile and do not show any adverse phenotype[8–10] making selective inhibition of PI3Kγ an attractive target for treatment of inflammatory and autoimmune disorders.

A number of publications have disclosed small molecules targeting PI3Kγ over the Class IA isoforms,[11,12] however thus far efforts in the pharmaceutical industry to develop drugs selectively targeting the PI3Kγ isoform have been unsuccessful. We have recently disclosed compounds **43** (CZC19945) and **53** (CZC24832) as potent PI3Kγ inhibitors with high selectivity over the other Class I isoforms.[13] This report details their discovery through optimization of HTS hits.

Screening of a kinase focused library[14] comprising 16,000 compounds in a high throughput chemoproteomics binding assay[13,15] identified the 6-aryl-[1,2,4]triazolo[1,5-a]pyrid-2-ylamines **1** and **2** as low micromolar hits for PI3Kγ with 5- to 10-fold selectivity over PI3Kδ and up to >30-fold selectivity over PI3Kα and PI3Kβ (Table 1).

We hypothesized that the exocyclic NH along with one of the nitrogen atoms in the triazolopyridine core could form the classical bi-dentate hydrogen bond donor-acceptor interaction with the hinge region of the kinase.[16,17] The pendant phenyl ring was identified as a suitable region for initial modification of the molecules, and a medicinal chemistry program was initiated to explore the SAR in this region.

Analogues at this position were readily accessible by means of a Suzuki reaction on the acetylated 6-bromo-[1,2,4]triazolo[1,5-a]pyrid-2-ylamine core **3**. This could be prepared from 2-amino-5-bromopyridine **4** in 4 steps[18] and allowed rapid access to analogues **5** enabling exploration of the SAR around the aryl ring. Modification of the synthesis by forming the boronic ester **6** allowed coupling with a wider variety of aryl bromides and chlorides (Scheme 1).[19] The acetyl group could be removed by treatment of **5** with acid to afford the amines **7**. Substitution of acetyl chloride with different electrophiles in step 1 allowed exploration of alternative groups on the exocyclic amine. Modification to the core could be achieved by use of alternative amino pyridines **4** as starting materials.

An array of molecules with diversely substituted phenyls was synthesized in the *N*-acetyl series. The set examined the effect of changing the regiochemistry and nature of functional group to

* Corresponding author.
E-mail address: ksmelt@onetel.com (K. Bell).

0960-894X/$ - see front matter © 2012 Elsevier Ltd. All rights reserved.
http://dx.doi.org/10.1016/j.bmcl.2012.06.049

Table 1
PI3Kγ hits from HTS

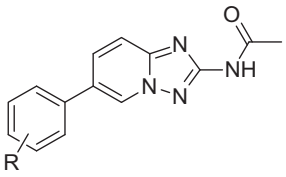

Compd #	R	PI3Kγ pIC_{50}	PI3Kδ pIC_{50}	PI3Kα pIC_{50}	PI3Kβ pIC_{50}
1	2-OMe	5.4	4.5	<4	<4
2	3,5-diMe,4-OH	5.7	5.2	4.9	4.7

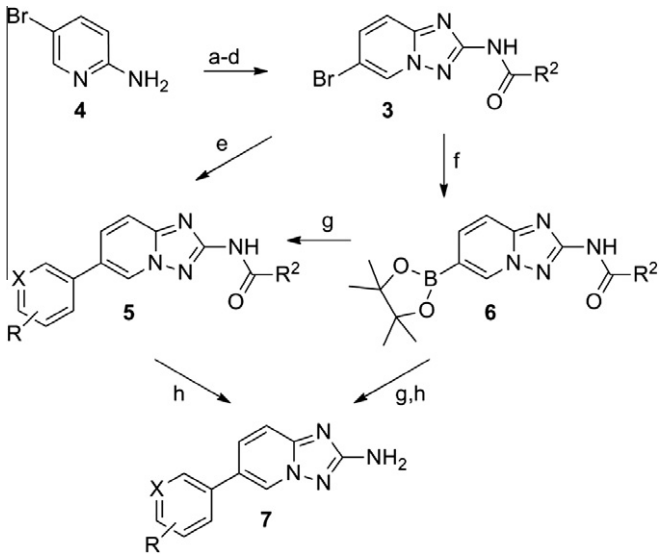

Scheme 1. Reagents and conditions: (a) EtOC(O)NCS, DCM, 5–20 °C, 16 h; (b) $NH_2OH{\cdot}HCl$, DIEA, EtOH, MeOH, 1 h rt then 2 h reflux; (c) CH_3COCl, Et_3N, 5–20 °C, 16 h; (d) NH_3, MeOH, rt, 16 h; (e) aryl-boronic acid, $Pd(dppf)_2Cl_2{\cdot}DCM$, Na_2CO_3, DME, H_2O, EtOH, 120 °C (μ-wave), 30 min; (f) Bis(pinacolato)diboron, toluene, $Pd(dppf)_2Cl_2{\cdot}DCM$, KOAc, 100 °C, 16 h; (g) Aryl bromide, $Pd(dppf)_2Cl_2{\cdot}DCM$, Na_2CO_3, DME, H_2O, EtOH, 120 °C (μ-wave), 30 min; (h) 4 M HCl in dioxane, rt, 18 h.

Table 2a
Inhibition of PI3Kγ/δ/α: aryls

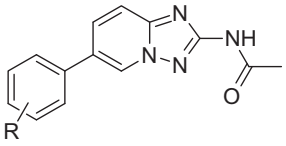

Compd #	R	PI3Kγ pIC_{50}	PI3Kδ pIC_{50}	PI3Kα pIC_{50}
8	3-OMe	6.8	<4.1	<4.1
9	4-OMe	6.0	4.5	4.6
10	3,4-diOMe	7.4	5.7	6.5
11	3-SO_2Me	6.3	5.5	<4.3
12	3-$NHSO_2$Me	6.5	5.3	5.3
13	3-SO_2NHMe	6.6	6.0	<5
14	3-CONHMe	6.2	<4	<4.3
15	4-SO_2Me	<4	<4	<4
16	4-SO_2NHMe	<4.3	<4	<4
17	3-SO_2NH^nBu	6.7	5.9	5.0
18	3-SO_2NHBn	6.3	5.2	<4
19	5-(3-Methyl)oxadiazole	<4.7	<4	NA
20	3-Ph	<5.4	<4	<4.7
21	3-SO_2NHBn,4-OMe	<4	<5	<4

explore the requirements of the binding pocket. Compounds were screened for binding affinity to PI3Kγ, along with the closest off-target PI3Kδ and the unwanted PI3Kα, using a chemoproteomic binding assay.[15] Cellular activity of the more potent compounds was assessed in a PI3Kγ-dependent cellular C5a-induced AKT Ser473 phosphorylation assay (pAKT) and an fMLP neutrophil migration assay (NeuMig).[13]

The 3-methoxy and 4-methoxy phenyl regioisomers **8** and **9** showed increased binding affinity for PI3Kγ compared to the screening hit **1**, whilst maintaining selectivity over the other PI3K isoforms (Table 2a). The 3,4-dimethoxy analogue, **10** was even more potent but showed a decrease in selectivity, particularly over the unwanted PI3Kα. When larger functional groups were investigated a clear preference was shown for C-3 rather than C-4 substitution. Sub-micromolar activity was achieved with methyl sulfones, sulfonamides and amides **11–14** at C-3 whereas the 4-substituted isomers **15** and **16** were completely inactive. Larger sulfonamides at C-3 such as *n*-butyl **17** and benzyl **18** could be accommodated in the binding pocket but did not increase PI3Kγ activity and as such afforded a decrease in the ligand efficiency of the molecules. Aromatic rings directly attached to C-3 such as the oxadiazole **19** and phenyl **20** were not tolerated suggesting that the vector of the group at this position was important for binding. Combination of the potent 3-sulfonamide with a 4-methoxy substituent, **21** afforded an inactive molecule.

A number of heterocyclic substituents at C-6 of the core were also explored (Table 2b). The 3-pyridine **22** was identified as a submicromolar inhibitor with greater than 60-fold selectivity over PI3Kδ and PI3Kα. Other heterocycles such as the pyrimidine **23** and isoquinoline **24** were around 10-fold less active as was the 4-pyridine **25**. A number of 5-membered heterocycles including dimethylthiazole **26** and pyrazole **27** were similarly 10- to 30-fold less active. The only other heterocycle tested which retained high affinity for PI3Kγ was thiophene, **28** but this analogue also showed high affinity for the unwanted PI3Kα. 5-substituted-3-pyridines in general increased binding affinity to PI3Kγ over the phenyl analogues (Table 2b). The 5-methoxy pyridine, **29** was around fivefold more potent than its aryl analogue and while the sulfone and sulfonamides **30–32** showed a 10- to 30-fold increase in potency.

A crystal structure of the pyridine sulfone **30** in PI3Kγ confirmed that it bound to the ATP binding pocket; the exocyclic NH and N-1 of the triazolopyridine formed a bi-dentate hydrogen bonding interaction with the protein backbone of Val882 in the hinge region of PI3Kγ (Fig. 1). The triazolopyridine core and pendant pyridine extended into a flat hydrophobic pocket achieving efficient binding by means of multiple hydrophobic contacts. A possible hydrogen bonding interaction was observed between the sulfone and catalytic lysine (Lys833). The acetyl group

Table 2b
Inhibition of PI3Kγ/δ/α: heterocycles

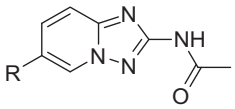

Compd #	R	PI3Kγ pIC_{50}	PI3Kδ pIC_{50}	PI3Kα pIC_{50}
22	Pyridin-3-yl	6.6	<4.5	4.8
23	Pyrimidin-5-yl	5.4	<4	<4.8
24	Isoquinolin-4-yl	5.5	<4	<4
25	Pyridin-4-yl	5.8	<4	5.8
26	2,4-Dimethylthiazol-5-yl	<4.9	<4	5.2
27	1-Methyl-1H-pyrazol-4-yl	5.4	<4.0	<4.2
28	Thiophen-3-yl	6.4	<4.7	6.7
29	5-Methoxypyridin-3-yl	7.2	<5	<5.4
30	5-(Methylsulfonyl)pyridin-3-yl	7.1	5.3	5.4
31	5-*N*-Benzylpyridine-3-sulfonamide	7.4	5.5	<5.5
32	5-(Methanesulfonamide)pyridin-3-yl	8.1	<6	<7

extended out towards solvent making it difficult to use the structure for exploration in this region.

Docking of **8** and **9** into a model built from the 4AOF crystal structure afforded a very similar binding mode to the native ligand, **30**. The small 4-methoxy substituent of compound **9** could be accommodated within the pocket and was able to make a similar hydrogen bonding interaction with Lys833 (Fig. 2).

In the case of the 4-sulfonamide **15** and 4-sulfone **16** the steric bulk of the larger groups forced the pendant phenyl ring out of the hydrophobic binding pocket resulting in reduced surface burial and hence lower binding affinity (Fig. 3). Docking of the 2-methoxyphenyl hit, compound **1**, showed that the increased dihedral angle between the phenyl ring and bicyclic core caused by the *ortho* substitution, forced the molecule away from the hinge relative to **30** thus accounting for the lower affinity for PI3Kγ.

Compound **30** exhibited high in vitro stability in human, rat and mouse microsomes with a half life >45 min in all species; however a rat PK study showed it to be rapidly cleared in vivo. Metabolic id studies in vivo on the related analogue **17** showed loss of the acetyl group to be a major metabolic pathway. As this group was not involved in any key binding interactions in **30** we reasoned that the amino analogue would retain binding affinity to PI3Kγ. The binding affinity of **33** to PI3Kγ was not significantly different from that of **30** (Table 3). Further analysis of the SAR on the RHS of the molecule showed that larger acyl groups such as cylcohexylamide maintained PI3Kγ affinity **34** but lost selectivity for PI3Kδ. Methylation of the NH **35** resulted in an inactive molecule, as expected from the crystal structure of **30**. Mono **36** and di-methylation **37** of **33** led to a reduction in PI3Kγ activity. A methylsulfonamide **38** was also prepared; however this was completely inactive against all Class I PI3K isoforms tested.

Testing of compounds **30** and **33** in the pAKT and neutrophil migration assays showed that the increased binding affinity conferred by the pyridine ring did not translate into a concomitant increase in cellular potency, the pyridine analogues being only marginally more active in cells than compound **11** (Table 4).

We postulated that the very low *c*log*P* values of **30** and **33** of −0.3 and −0.4, respectively may be limiting the cellular permeability. A further array of analogues was prepared in the 2-amino series, increasing lipophilicity of the R^1 substituent with the aim of

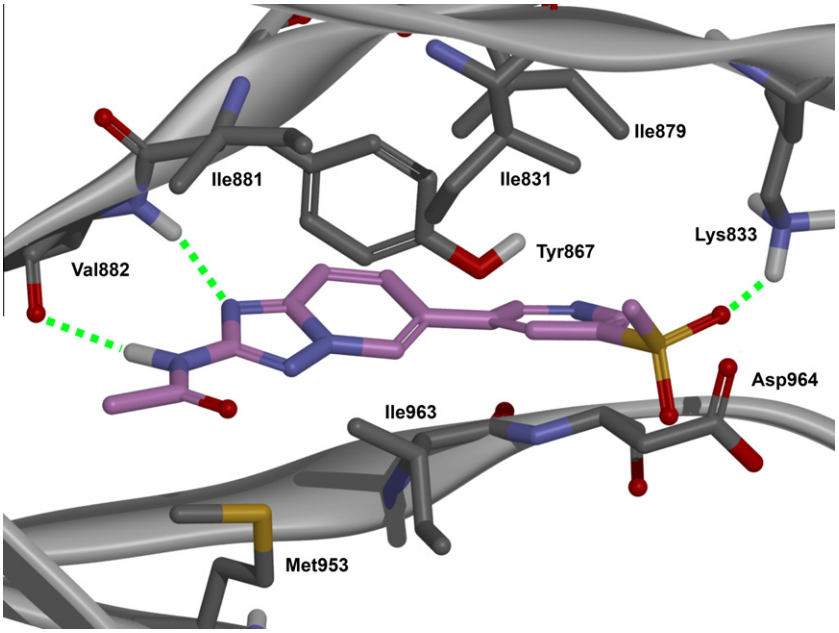

Figure 1. Crystal structure of **30** in PI3Kγ (PDB code 4AOF). Hydrogen bonding interactions between the hinge and **30**; and Lys833 and **30** are depicted by dashed lines.

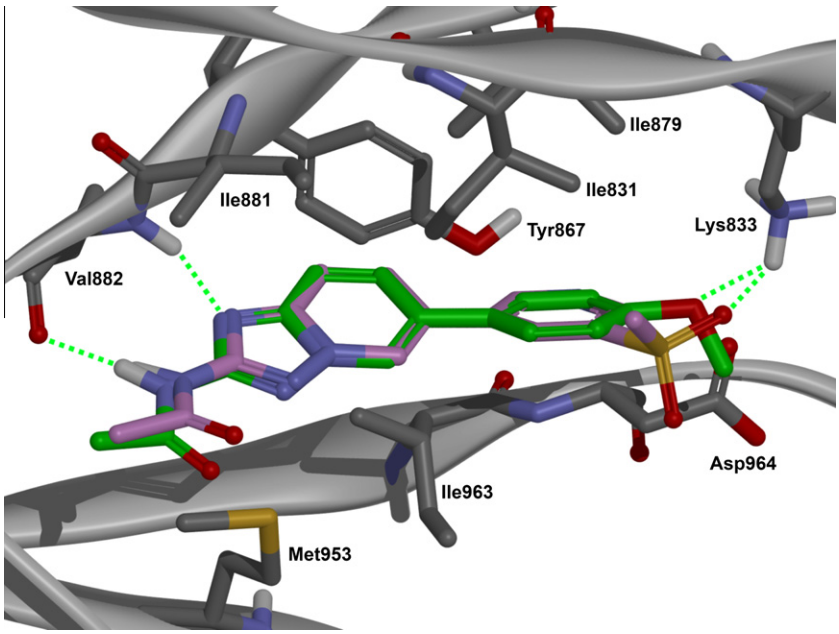

Figure 2. Docking of compound **9** (green) into 4AOF, overlaid with the native ligand, compound **30** (pink).

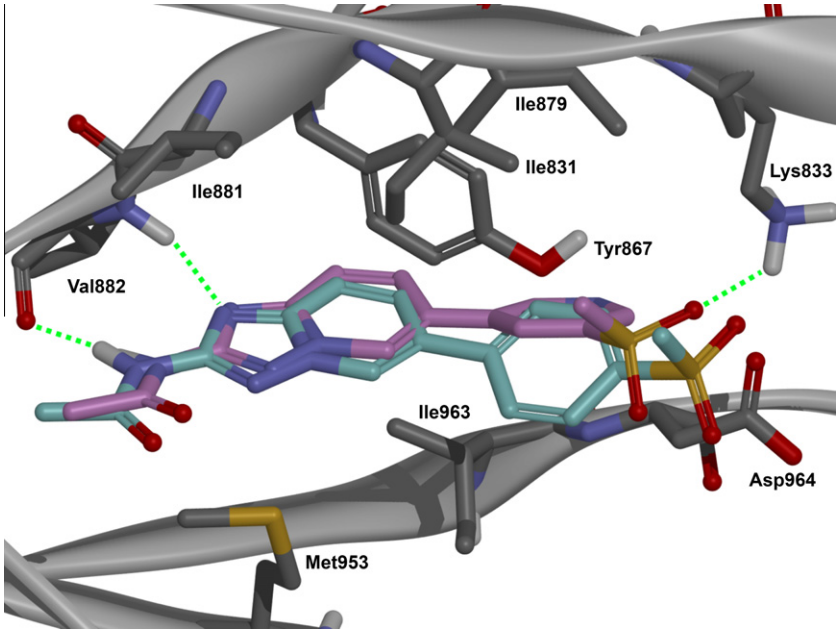

Figure 3. Docking of compound **15** (blue) 4AOF, overlaid with the native ligand, compound **30** (pink). Compound **15** no longer makes optimal hydrophobic interactions with the binding pocket.

improving cellular permeability (Table 5). N-linked and S-linked sulfonamides were chosen for initial investigations in preference to the sulfones as synthetic tractability enabled a more rapid exploration of the SAR. The lipophilic N-linked aryl sulfonamides **39** and **40** afforded highly potent PI3Kγ binding and showed promising activity in the pAKT assay however low activity was observed in the neutrophil migration assay possibly attributable to high plasma protein binding (>99%). The S-linked aryl sulfonamides **41** and **42** showed only weak PI3Kγ binding; however the S-linked alkyl sulfomanides **43–45** showed intermediate PI3Kγ binding affinity and in the case of **43** and **44** sub-micromolar cellular activity in the neutrophil migration assay. The best alkyl-sulfonamides groups were prepared as their sulfone analogues; however they were typically less potent such as the *tert*-butyl sulfone **46** which was almost 10-fold less potent that **43**.

Modeling studies of **43** suggested that this may be due to a potential hydrogen bonding interaction between the NH of the sulfonamide and conserved Asp964 of the DFG unit which cannot be achieved in the sulfones (Fig. 4). In addition the docking mode also showed a potential hydrogen bonding interaction between the pyridine nitrogen and side chain of Tyr867 not present in the crystal structure of compound **30**.

Both the *tert*-butylsulfonamide **43** and *iso*-propylsulfonamide **44** showed high stability in human, mouse and rat microsomes with a half life >45 min in all species. **43** was further characterized using mass spectrometry based profiling against a panel of

Table 3
Inhibition of PI3Kγ/δ/α: RHS

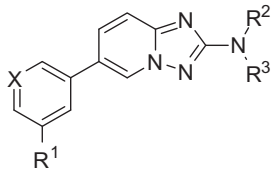

Compd #	R^1	X	R^2	R^3	PI3Kγ pIC_{50}	PI3Kδ pIC_{50}	PI3Kα pIC_{50}
30	SO_2Me	N	H	Ac	7.1	5.3	5.4
33	SO_2Me	N	H	H	7.0	5.2	5.0
34	$NHSO_2Me$	CH	H	CO(cyclohexyl)	6.5	6.3	<4
35	SO_2Me	CH	Me	Ac	<4.5	<4	<4
36	SO_2Me	N	H	Me	6.5	<4.6	<5.4
37	SO_2Me	N	Me	Me	5.5	<4	<4
38	SO_2Me	N	H	SO_2Me	<4.4	<4	<4

Table 4
Cellular data

Compd #	PI3Kγ pIC_{50}	pAKT pIC_{50}	NeuMig pIC_{50}
11	6.3	<4.9	5.4
30	7.1	<4.2	5.7
33	7.0	5.7	5.7

kinases.[20] High selectivity was observed across the protein kinases; however the compound was shown to have only 10-fold selectivity over PI3Kβ.[21]

We explored the SAR around the [1,2,4]triazolo[1,5-a]pyridine core by addition of methyl groups in the 5, 7 and 8 positions to identify where substituents could be tolerated in order to further modify the physical properties of the molecules. Methyl groups were tolerated at C-8 **47** but not *ortho* to the pyridyl ring at C-7 **48** or C-5 **49** (Table 6). This fitted with our binding hypothesis for compound **1** in which *ortho* substituents increase dihedral angle between the bicyclic core and pyridyl ring meaning the molecule cannot not be readily accommodated in the binding pocket. Lipophilic substituents were subsequently explored at C-8 position with the aim of increasing cellular permeability. The more lipophilic groups, trifluoromethyl **50** and chloro **51** resulted in a loss of binding activity; however the 8-fluoro analogue **52** retained sub micromolar activity. The fluorine was combined with our preferred *tert*-butyl sulfonamide to afford **53.** The addition of the fluorine did not increase cellular potency however the molecule did show unexpected improved selectivity over PI3Kβ. The 7-fluoro analogue **54** was completely inactive despite the fact that fluorine is not generally considered large enough to force an increase in the dihedral angle between two aromatic rings.

High microsomal stability and good Caco2 data for **43** and **53** translated to low clearance and high bioavailability in a rat in vivo PK study (Table 7); In addition compound **43** and **53** showed no inhibition in a hERG assay up to 100 μM,[22] nor CYP inhibition up to 25 μM for CYP1A, 2C19, 2C9, 2D6 and 3A4 and were negative in an Ames assay.[23]

When evaluated in a mouse Collagen Induced Arthritis (CIA) model **43** and **53** significantly reduced the severity and development of arthritis. Mice treated orally with 10 mg/kg test compound showed a reduction in the average clinical score of 53% and 38% for **43** and **53**, respectively.[13,24] **53** exhibited poor thermodynamic solubility (<5 μg/mL) and its measured pKa's of 11 and 1.4 precluded salt formation which made pre-clinical development problematic; however **43** showed improved solubility (9 μg/mL) and its calculated pKa's of 10 and 4.2[25] suggested that salt formation would be feasible and thus despite its limited PI3Kβ selectivity it may have potential for further development as a PI3Kγ inhibitor.

In summary, we have described the identification and SAR around a new class of PI3Kγ inhibitors. The 6-aryl triazolopyridines **43** (CZC19945) and **53** (CZC24832) have been shown to be potent inhibitors of PI3Kγ with good in vivo PK profile and have demonstrated efficacy in a chronic model of inflammation. Both compounds show high selectivity over PI3Kα and **53** is almost 100-fold selective over PI3Kβ and PI3Kδ, making them important compounds for investigating the effects of inhibiting the various Class I PI3Ks in vivo.

Table 5
Inhibition of PI3Kγ/δ/α, cellular data and *c*log*P* vaules: amines

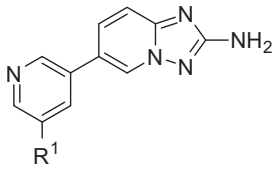

Compd #	R^1	PI3Kγ pIC_{50}	PI3Kδ pIC_{50}	PI3Kα pIC_{50}	pAKT pIC_{50}	NeuMig pIC_{50}	*c*log*P*
39	Naphthalene-1-sulfonamide	8.1	6.9	<7.0	6.3	4.7	2.8
40	$NHSO_2$(4-ClPh)	8.2	6.4	6.8	5.7	4.8	2.5
41	SO_2NH(4-ClPh)	6.2	5.2	5.4	<4.9	NA	2.9
42	SO_2NHBn	6.6	5.1	<4.7	5.9	5.1	2.2
43	SO_2NH^tBu	7.6	5.8	5.6	5.7	6.0	1.7
44	SO_2NH^iPr	7.5	5.8	5.6	5.8	6.2	1.3
45	SO_2NHCH_2Cyclopropyl	7.8	<5.2	5.5	5.7	5.8	1.4
46	$SO_2{}^tBu$	6.8	5.5	<4.8	<5	NA	0.8

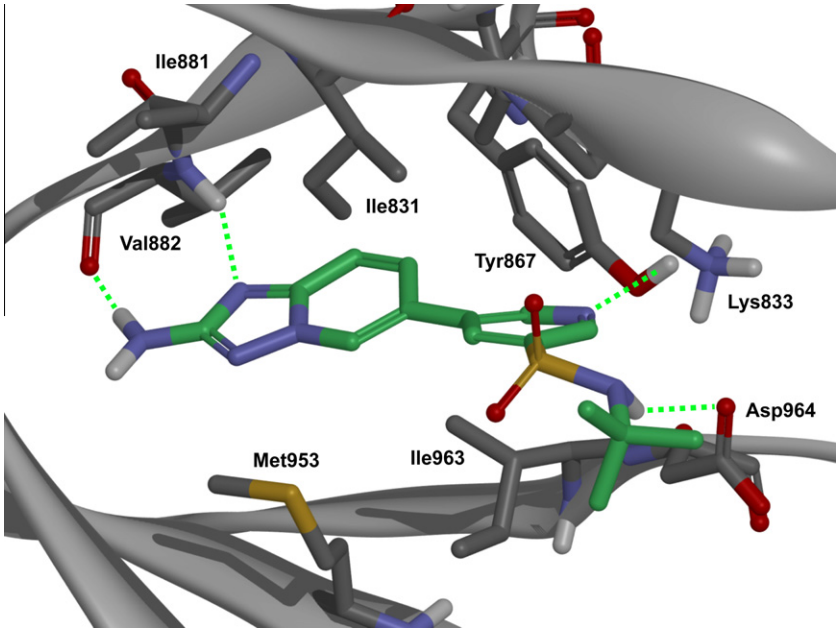

Figure 4. Docking of compound **43** into PI3Kγ (4AOF). Hydrogen bonding interactions are shown with dashed lines.

Table 6
Inhibition of PI3Kγ/δ/α/β: core substituents

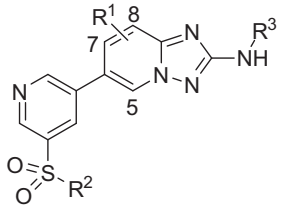

Compd #	R^1	R^2	R^3	PI3Kγ pIC_{50}	PI3Kδ pIC_{50}	PI3Kα pIC_{50}	PI3Kβ pIC_{50}
47	8-Me	Me	Ac	7.0	<5.3	<4.4	4.7
48	7-Me	Me	Ac	<4	<4	<4	3.7
49	5-Me	Me	Ac	6.0	<4.4	<4	4.6
50	8-CF_3	Me	H	<4	<4	<4	NA
51	8-Cl	Me	H	5.7	<4	<4	<4
52	8-F	Me	Ac	6.9	<4.7	<4.7	4.7
53	8-F	NH^{t}Bu	H	7.6	5.1	<5	5.9
54	7-F	NH^{t}Bu	H	4.6	<4	<4	<4

Table 7
Pharmacokinetic parameters of **43** and **53**

Id	Cl mL/min/kg	*F*%
43[a]	11.5	88
53[b]	14	37

[a] 1 mg/kg iv and 5 mg/kg po
[b] 0.2 mg/kg iv and 10 mg/kg po

Acknowledgements

We are grateful to the biology and biochemistry groups for assay development and screening, Thilo Werner and the MS group for compound profiling; Dave Middlemiss for medicinal chemistry advice and Tammy Ladduwahetty for advice on the preparation of the manuscript.

References and notes

1. Vanhaesebroeck, B.; Guillermet-Guibert, J.; Graupera, M.; Bilanges, B. *Nat. Rev. Mol. Cell Biol.* **2010**, *11*, 329.
2. Hawkins, P. T.; Anderson, K. E.; Davidson, K.; Stephens, L. R. *Biochem. Soc. Trans.* **2006**, *34*, 647.
3. Bohnacker, T.; Marone, R.; Collmann, E.; Calvez, R.; Hirsch, E.; Wymann, M. *Sci. Signal.* **2009**, *2*, ra27.
4. Ghigo, A.; Damilano, F.; Braccini, L.; Hirsch, E. *BioEssays* **2010**, *32*, 185.
5. Knight, Z. A.; Gonzales, B.; Feldman, M. E.; Zunder, E. R.; Goldenberg, D. D.; Williams, O.; Loewith, R.; Stokoe, D.; Balla, A.; Toth, B.; Balla, T.; Weiss, W. A.; Williams, R. L.; Shokat, K. M. *Cell* **2006**, *125*, 733.
6. Bi, L.; Okabe, I.; Bernard, D. J.; Wynshaw-Boris, A.; Nussbaum, R. L. *J. Biol. Chem.* **1999**, *274*, 10963.
7. Bi, L.; Okabe, I.; Bernard, D. J.; Nussbaum, R. L. *Mamm. Genome* **2002**, *13*, 169.
8. Sasaki, T.; Irie-Sasaki, J.; Jones, R. G.; Oliveira-dos-Santos, A. J.; Stanford, W. L.; Bolon, B.; Wakeham, A.; Itie, A.; Bouchard, D.; Kozieradzki, I.; Joza, N.; Mak, T. W.; Ohashi, P. S.; Suzuki, A.; Penninger, J. M. *Science* **2000**, *1040*, 287.
9. Hirsch, E.; Katanaev, V. L.; Garlanda, C.; Azzolino, O.; Pirola, L.; Silengo, L.; Sozzani, S.; Mantovani, A.; Altruda, F.; Wymann, M. *Science* **2000**, *1049*, 287.
10. Li, Z.; Jiang, H.; Xie, W.; Zhang, Z.; Smrcka, A. V.; Wu, D. *Science* **2000**, *1046*, 287.
11. Pomel, V.; Klicic, J.; Covini, D. D.; Church, D.; Shaw, J. P.; Roulin, K.; Burgat-Charvillon, F.; Valognes, D.; Camps, M.; Chabert, C.; Gillieron, C.; Françon, B.; Perrin, D.; Leroy, D.; Gretener, D.; Nichols, A.; Vitte, P. A.; Carboni, S.; Rommel, C.; Schwarz, M. K.; Rückle, T. *J. Med. Chem.* **2006**, *49*, 3857.
12. Ameriks, M. K.; Venable, J. D. *Curr. Top. Med. Chem.* **2009**, *9*, 738.
13. Bergamini, G.; Bell, K.; Shimamura, S.; Werner, T.; Cansfield, A.; Müller, K.; Perrin, J.; Rau, C.; Ellard, K.; Hopf, C.; Doce, C.; Leggate, D.; Mangano, R.; Mathieson, T.; O'Mahony, A.; Plavec, I.; Rharbaoui, F.; Reinhard, F.; Savitski, M. M.; Ramsden, N.; Hirsch, E.; Drewes, G.; Rausch, O.; Bantscheff, M.; Neubauer, G. *Nat. Chem. Biol.* **2012**, *8*, 576.

14. The hits **1** and **2** were included in a library purchased from BioFocus.
15. Bergamini, G.; Cansfield, A.; Ramsden, N.; Neubauer, G. PCT Int. Appl. WO2008015013.
16. Liao, J-L. L. *J. Med. Chem.* **2007**, *50*, 409.
17. Backes, A. C.; Zech, B.; Felber, B.; Klebl, B.; Müller, G. *Expert Opin. Drug Discov.* **2008**, *3*, 1409.
18. Wilson, F.; Ramsden, N.; Bell, K.; Cansfield, A.; Burckhardt, S.; Taylor, J.; Sunose, M.; Middlemiss, D. PCT Int. Appl. WO2008025821.
19. Ramsden, N.; Bell, K.; Cansfield; Taylor, J.; Sunose, M.; Middlesmiss, D.; Neubauer, G. PCT Int. Appl. WO2009068482.
20. Bantscheff, M.; Eberhard, D.; Abraham, Y.; Bastuck, S.; Boesche, M.; Hobson, S.; Mathieson, T.; Perrin, J.; Raida, M.; Rau, C.; Reader, V.; Sweetman, G.; Bauer, A.; Bouwmeester, T.; Hopf, C.; Kruse, U.; Neubauer, G.; Ramsden, N.; Rick, J.; Kuster, B.; Drewes, G. *Nat. Biotechnol.* **2007**, *1035*, 25.
21. Compound **44** was tested against an off-target panel which includes >150 kinases and other proteins. Lipid kinases: PIP4K2C, PIP4K2A and PI3Kβ <30-fold; Protein kinases: AAK1 <100-fold.
22. Herg testing was performed at Neurosolutions, Cambridge in a Q-patch assay.
23. Neither toxicity nor mutagenic activity has been observed at 1667 μg/plate (compound precipitation observed at higher concentrations) in 3 Samonella typhimurium strains (TA100, TA1537, TA98 ± liver S9 fraction).
24. The Collagen Induced Arthritis (CIA) mouse model was carried out at Bolder BioPath (Colorado). Male mice of DBA/B10 strain were injected intradermally with bovine type II collagen at day 0 (boost at day 21). Mice develop inflammation 3–5 weeks after the first collagen injection. A chronic inflammation in the joints of the animals is achieved within 7–10 days after disease onset. The quantification of the clinical inflammation is done by scores (0–5) which combines the measurement of the volume of several body parts, for example digits, hind and fore limbs (pads and ankles/wrists swelling). The compound was administered orally twice per day every 12 h (po, bid).
25. Calculation using ACD labs software.